Intermolecular Triple Proton and Deuteron Transfer in Crystalline 3,5-Dimethylpyrazole Studied by NMR, NQR, and X-ray Methods

John A. S. Smith,*[1e] Bernd Wehrle,[1a] Francisco Aguilar-Parrilla,[1a] Hans-Heinrich Limbach,*[1a] Maria de la Concepción Foces-Foces,[1b] Felix Hernández Cano,[1b] José Elguero,[1c] André Baldy,[1d] Marcel Pierrot,[1d] Mian M. T. Khurshid,[1e] and Jacqueline B. Larcombe-McDouall[1e]

Contribution from the Institut für Physikalische Chemie der Universität Freiburg i.Br., Albertstrasse 21, D-7800 Freiburg, West Germany, the U.E.I. de Cristallografía, Instituto de Química Física "Rocasolano", Serrano 119, E-28006 Madrid, Spain, the Instituto de Química Médica, C.S.I.C., Juan de la Cierva 3, E-28006 Madrid, the Service de Cristallochimie, Université d'Aix-Marseille III, Avenue Escadrille Normandie-Niemen, F-13397 Marseille-Cedex 13, France, and the Department of Chemistry, King's College, Strand, London WC2R 2LS, United Kingdom. *Received September 21, 1988*

Abstract: A combination of ^{13}C, ^{15}N magnetic resonance, ^{14}N quadrupole double resonance, and X-ray studies of solid 3,5-dimethylpyrazole between 270 and 350 K has shown that the NH···N hydrogen bond units present in the crystal are dynamically disordered, so that each nitrogen atom is on average attached to half a hydrogen atom. The molecules form discrete hydrogen-bonded cyclic trimers, in which the hydrogen atoms move in a double minimum potential energy surface which is symmetrical, to within experimental error. The experimental evidence in this temperature range is consistent with disorder by means of correlated triple hydrogen jumps with an activation energy of 45 kJ mol^{-1}. There is a large kinetic hydrogen (HHH)/deuterium (DDD) isotope effect of >20 at 299 K and equal to 8 at 347 K.

Despite the numerous studies that have been published of proton tautomerism of simple azoles in liquid solution,[2-6] little is known about the mechanism of these processes. Thus, the number of azole molecules participating in the exchange, i.e., the number of protons exchanging, has not yet been established. Since major molecular motions such as diffusion and hydrogen bond exchange are suppressed in the solid state, the study of azole tautomerism in molecular crystals where the hydrogen bond network is fixed is of special importance. Early X-ray and neutron diffraction studies, which are clearly sensitive to proton disorder in the solid state, showed proton order in crystalline pyrazole,[7-9] imidazole,[10] 1,2,4-triazole,[11,12] tetrazole,[13] which means that of two potential tautomers only one is detected in these crystals in contrast to the liquid state. Unfortunately, diffraction studies yield "occupation numbers" for distinguishable proton sites and little information on the dynamics and the mechanism of the proton tautomerism.

Chart I

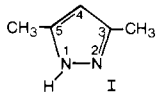

I

Ia ; I - $^{15}N_2H$

Ib ; I - $^{15}N_2D$

Thus, the presence of small amounts of nondominating tautomers can be easily missed by these methods. It is, therefore, important to use in addition nuclear magnetic resonance methods to study the problem of solid-state proton tautomerism. The method which allows us to see very quickly whether or not dynamic processes in solid organic molecules are present is certainly high-resolution solid-state ^{13}C NMR spectroscopy under conditions of ^{1}H-^{13}C cross-polarization (CP), ^{1}H decoupling, and magic angle spinning (MAS).[14,15] This technique has already been used to show the absence of disorder in crystalline pyrazole and imidazole at room temperature,[16] results which are also consistent with their ^{14}N quadrupole double resonance spectra.[17,18] The same method[19] has been used to confirm the absence of proton tautomerism in a number of other substituted azoles, a recent exception being found in the case of 3,5-dimethylpyrazole, I.[20] Preliminary ^{13}C CPMAS experiments revealed a temperature-dependent dynamic process attributed to a solid-state proton transfer.[20] This exceptional behavior was paralleled by the X-ray structure analysis which showed that I forms cyclic trimers in the solid state. Rate constants of this process could not, however, be obtained in these

(1) (a) Universität Freiburg. (b) Instituto "Rocasolano", Madrid. (c) C.S.I.C. Madrid. (d) Université Aix-Marseille III. (e) King's College, London.

(2) Elguero, J.; Marzin, C.; Katrizky, A. R.; Linda, P. *The Tautomerism of Heterocycles*; Academic Press: New York, 1976; pp 266-325.

(3) (a) Nesmeyanov, A. N.; Zavelovitch, E. B.; Babin, V. N.; Kochetkova, N. S.; Fedin, E. I. *Tetrahedron* **1976**, *31*, 1461-1462. (b) Nesmeyanov, A. N.; Babin, V. N.; Zavelovitch, E. B.; Kochetkova, N. S.; Fedin, E. I. *Chem. Phys. Lett.* **1976**, *37*, 184-186.

(4) Litchman, W. M. *J. Am. Chem. Soc.* **1979**, *101*, 545-547.

(5) Chenon, M. T.; Coupry, C.; Grant, D. M.; Pugmire, R. *J. Org. Chem.* **1977**, *42*, 659-661.

(6) Limbach, H. H. The Use of NMR Spectroscopy in the Study of Hydrogen Bonding in Solution, In *Aggregation Processes*; Gormally, J., Wyn-Jones, E., Eds.; Elsevier: Amsterdam, 1983; Chapter 16, p 1982.

(7) Berthou, J.; Elguero, J.; Rérat, C. *Acta Crystallogr. Sect. B* **1970**, *26*, 1880-1881.

(8) La Cour, T.; Rasmussen, W. E. *Acta Chem. Scand.* **1973**, *27*, 1845-1854.

(9) Larsen, F. K.; Lehmann, M. S.; Sotofte, I.; Rasmussen, W. E. *Acta Chem. Scand.* **1970**, *24*, 3248-3258.

(10) Martinez-Carrera, S. *Acta Crystallogr.* **1976**, *20*, 783-789.

(11) Goldstein, P.; Ladell, J.; Abowitz, G. *Acta Crystallogr. Sect. B* **1969**, *25*, 135-143.

(12) Jeffrey, G. A. *Theochem.* **1984**, *17*, 1-15. Jeffrey, G. A.; Ruble, J. R.; Yates, J. H. *Acta Crystallogr. Sect. B* **1983**, *39*, 388-394.

(13) Putten, N. V.; Heijdenrijk, D.; Schenk, M. *Cryst. Struct. Commun.* **1974**, *3*, 321-322.

(14) Schaeffer, J.; Stejskal, E. O. *J. Am. Chem. Soc.* **1976**, *98*, 1031-1032.

(15) Lyerla, J. R.; Yannoni, C. S.; Fyfe, C. A. *Acc. Chem. Res.* **1982**, *15*, 208-216.

(16) (a) Elguero, J.; Fruchier, A.; Pellegrin, V. *J. Chem. Soc., Chem. Commun.* **1981**, 1207-1208. (b) Munowitz, M.; Bachovchin, W. W.; Herzfeld, J.; Dobson, C. M.; Griffin, R. G. *J. Am. Chem. Soc.* **1982**, *104*, 1192-1196.

(17) Palmer, M. H.; Scott, F. E.; Smith, J. A. S. *Chem. Phys.* **1983**, *74*, 97.

(18) Palmer, M. H.; Stephenson, D.; Smith, J. A. S. *Chem. Phys.* **1985**, *97*, 103-111.

(19) Faure, R.; Vincent, E. J.; Rousseau, A.; Clarmunt, R. M.; Elguero, J. *Can. J. Chem.* **1988**, *66*, 1141-1146.

(20) Baldy, A.; Elguero, J.; Faure, R.; Pierrot, M.; Vincent, E. J. *J. Am. Chem. Soc.* **1985**, *107*, 5290-5291.

0002-7863/89/1511-7304$01.50/0

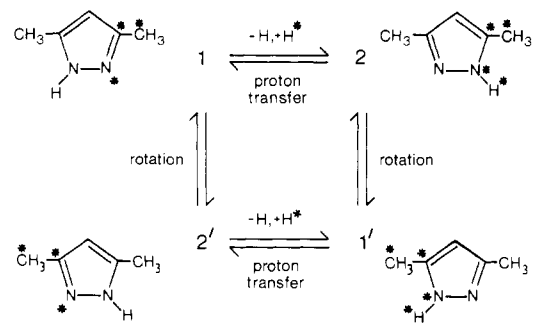

Figure 1. Proton transfer vs 180° rotation in solid 3,5-dimethylpyrazole (I).

preliminary experiments, leaving open the question of the actual nature of the proton-transfer process. Thus, a priori, the observed phenomena can be explained either by a correlated triple proton transfer or by correlated 180° rotations of the pyrazole molecules followed by a proton transfer as indicated in Figure 1 or both acting simultaneously. Evidence for such rotations has been found, for example, in the related case of solid tropolone.[21] Furthermore, the question as to whether or not the reaction involves kinetic hydrogen/deuterium isotope effects has not yet been studied nor the possible effects on the spectra of small nonaveraged dipolar coupling to ^{14}N or ^{2}H.[22]

In order to try to answer these questions we have studied the solid-state tautomerism of I with use of several NMR methods of which the results are reported in this paper. In addition to ^{13}C NMR and ^{14}N quadrupole double resonance spectroscopy mentioned above we have employed also ^{15}N CPMAS spectroscopy of ^{15}N-labeled I. This method has been shown to be particularly useful when studying solid-state proton tautomerism involving nitrogen atoms.[23-28] The method covers in an ideal way the dynamic gap between ^{13}C and ^{14}N spectroscopy. Thus, we report here rate constants for the tautomerism of crystalline I, together with experiments on the same molecule deuterated at the NH sites to show that the reaction involves a substantial kinetic hydrogen/deuterium isotope effect. These experiments are described in the experimental section and are followed by an analysis and discussion of the results in terms of a triple proton transfer in the cyclic hydrogen-bonded trimer of I.

Experimental Section

Materials. The materials studied are shown in Chart I. Samples of 3,5-dimethylpyrazole (I) were obtained from Aldrich, and their purity was checked by mass and NMR spectroscopy. 3,5-Dimethylpyrazole-$^{15}N_2$ (Ia) was synthesized according to procedures reported in the literature[29] starting from hydrazine sulfate-$^{15}N_2$ (AH GmbH, Düsseldorf). 3,5-Dimethylpyrazole-$^{15}N_2$-d_1 (Ib) deuterated on N(1) was prepared by deuteration of Ia by using a vacuum line and CH_3OD as the deuterating agent.

^{14}N Quadrupole Double Resonance Experiments. The ^{14}N quadrupole resonance experiments were conducted on a variable temperature field cycling spectrometer in which the magnetic field was varied by mechanical transport of the sample.[30] Fuller details of this instrument will be published elsewhere;[31] the temperature of the sample could be varied between 220 and 370 K by means of a cooled or heated stream of nitrogen or air, which also served to transport mechanically the sample from the high-to-low field coils. The temperature of the stream was continuously monitored and could be used for control purposes by means of an Oxford Instruments DTC-2 controller. The temperature of the sample, however, always differed from this reading, this difference being calibrated by recording ^{35}Cl quadrupole double resonance frequencies in *p*-chlorobenzoic acid, the temperature dependence in which had been previously measured on a "Decca" super-regenerative oscillator spectrometer.

The ^{14}N quadrupole resonance frequencies were recorded by both level-crossing[30] and cross relaxation[32] methods; in the latter, the cross relaxation field was calibrated and converted to frequency by recording low-field ^{1}H magnetic resonance in $Te(OH)_6$ at various currents to the cross-relaxation solenoid. The temperature measurements were accurate to about ±2 K and those of frequency to about ±20 kHz.

^{13}C CPMAS NMR Experiments. The ^{13}C CPMAS NMR spectra of 3,5-dimethylpyrazole (I) were recorded on a 7.1 T Bruker CXP-300 spectrometer at a frequency of 75.5 MHz as described previously.[20]

^{15}N CPMAS NMR Measurements. All ^{15}N CPMAS NMR experiments were performed on a Bruker CXP 100 pulse FT NMR spectrometer working at 90.02 MHz for protons and at 9.12 MHz for ^{15}N. The spectrometer is equipped with an 2.1 T electromagnet (gap size of 2.2 cm). The experiments were performed with a Doty MAS probe[33] adapted for a small magnet gap size. For the longterm stability of the magnetic field and low-temperature operation, a toluene-d_8 ^{2}H lock was used which could be located near the sample. The rotors had an outer diameter of 5 mm and a length of 1 cm and contained about 50 mg material. Low-temperature operation of the magic-angle spinner assembly was achieved by using cold nitrogen as the driving gas. For this purpose a homebuilt heat exchanger was used, which has been described previously[23b] and which avoids liquefaction of the nitrogen spinning gas when liquid nitrogen is used as a cooling medium.

After Fourier transformation, the NMR spectra were transferred to a Olivetti M 28 personal computer and to the Rechenzentrum der Universität Freiburg where the line shape analysis was carried out as described previously.[25-27]

NMR and NQR Line Shape Analysis. In this section we define the kinetic and thermodynamic parameters of two-state chemical exchange processes which are obtained from the analysis of solid-state NMR and NQR spectra.

Let us consider a molecule exchanging between two unequally populated states **1** and **2** characterized by the probabilities x_1 and x_2 and by the equilibrium constant

$$K_{12} = x_2/x_1 = k_{12}/k_{21} \quad (1)$$

where k_{12} and k_{21} are the rate constants of the exchange. Let the molecule contain two uncoupled spins A and X giving rise to the NMR transitions ν_{A1}, ν_{A2}, ν_{X1}, and ν_{X2}, where the subscript indicates the molecular state. The exchange problem can then be formulated in terms of two superposed independent asymmetric two-state exchange systems A and X, for which the exchange-broadened line shapes can easily be calculated.[34-36] Results of such calculations have been presented recently.[28] If in the slow-exchange regime each spin system contributes two lines to the spectrum, four lines appear at the positions ν_{A1}, ν_{A2}, ν_{X1}, and ν_{X2}. The line intensity ratios A_2/A_1 and X_2/X_1 correspond to the equilibrium constant K_{12}. As k_{12} is increased the lines broaden and coalesce. The position of the averaged lines is given by

$$\nu_S = x_1\nu_{S1} + (1 - x_1)\nu_{S2}, \qquad S = A, X \quad (2)$$

(21) Szeverenyi, N. M.; Bax, A.; Maciel, G. E. *J. Am. Chem. Soc.* **1983**, *105*, 2579-2582.

(22) (a) Hexem, J. G.; Frey, M. H.; Opella, S. J. *J. Chem. Phys.* **1982**, *77*, 3847-3856. (b) Olivieri, A. C.; Frydman, L.; Diaz, L. E. *J. Magn. Reson.* **1987**, *75*, 50-62. (c) Olivieri, A. C.; Frydman, L.; Graselli, M.; Diaz, L. E. *Mag. Res. Chem.* **1988**, *26*, 615-618. (d) Swanson, S. D.; Ganapathy, S.; Bryant, R. G. *J. Magn. Reson.* **1987**, *73*, 239-243.

(23) (a) Limbach, H. H.; Hennig, J.; Kendrick, R. D.; Yannoni, C. S. *J. Am. Chem. Soc.* **1984**, *106*, 4059-4060. (b) Kendrick, R. D.; Friedrich, S.; Wehrle, B.; Limbach, H. H.; Yannoni, C. S. *J. Magn. Reson.* **1985**, *65*, 159-161.

(24) (a) Frydman, L.; Olivieri, A. C.; Diaz, L. E.; Frydman, B.; Morin, F. G.; Mayne, C. L.; Grant, D. M.; Adler, A. D. *J. Am. Chem. Soc.* **1988**, *110*, 336-342. (b) Frydman, L.; Olivieri, A. C.; Diaz, L. E.; Valasimas, A.; Frydman, B. *J. Am. Chem. Soc.* **1988**, *110*, 5651-5661.

(25) (a) Limbach, H. H.; Wehrle, B.; Zimmermann, H.; Kendrick, R. D.; Yannoni, C. S. *J. Am. Chem. Soc.* **1987**, *109*, 929-930. (b) Limbach, H. H.; Wehrle, B.; Zimmermann, H.; Kendrick, R. D.; Yannoni, C. S. *Angew. Chem.* **1987**, *99*, 241-243; *Angew. Chem., Int. Ed. Engl.* **1987**, *26*, 247-248.

(26) Wehrle, B.; Limbach, H. H.; Köcher, M.; Ermer, O.; Vogel, E. *Angew. Chem.* **1987**, *99*, 914-917; *Angew. Chem., Int. Ed. Engl.* **1987**, *26*, 934-936.

(27) (a) Wehrle, B.; Limbach, H. H.; Zimmermann, H. *Ber. Bunsenges. Phys. Chem.* **1987**, *91*, 941-950. (b) Wehrle, B.; Zimmermann, H.; Limbach, H. H. *J. Am. Chem. Soc.* **1988**, *110*, 7014-7024.

(28) (a) Limbach, H. H.; Wehrle, B.; Schlabach, M.; Kendrick, R. D.; Yannoni, C. S. *J. Magn. Reson.* **1988**, *77*, 84-100. (b) Wehrle, B.; Limbach, H. H. *Chem. Phys.*, in press.

(29) Wiley, R. H.; Hexner, P. E. *Org. Synth. Collect.* **1963**, *4*, 351-353.

(30) Edmonds, D. T. *Phys. Rep. C.* **1977**, *29*, 233-290.

(31) Larcombe-McDouall, J. B.; Smith, J. A. S. *J. Chem. Soc., Faraday Trans. 2* **1989**, *85*, 53-64.

(32) Stephenson, D.; Smith, J. A. S. *Proc. Roy. Soc. London Ser. A* **1988**, *416*, 149-178.

(33) Doty, F. D.; Ellis, P. D. *Rev. Sci. Instrum.* **1981**, *52*, 1868-1875.

(34) (a) Gutowsky, H. S.; McCall, D. W.; Slichter, C. P. *J. Chem. Phys.* **1953**, *21*, 279-292. (b) Kubo, R. *Nuovo Cimento, Suppl.* **1957**, *6*, 1063. Sack, R. A. *Mol. Phys.* **1958**, *1*, 163-167.

(35) Lyerla, J. R.; Yannoni, C. S.; Fyfe, C. A. *Acc. Chem. Res.* **1982**, *15*, 208-216.

(36) Binsch, G. *J. Am. Chem. Soc.* **1969**, *91*, 1304-1309.

Table I. Final Fractional Atomic Coordinates[a]

	x	y	z
C(4)	0.6464	0.0	0.25
C(3)	0.7697	0.1073	0.2512
N(2)	0.8540	0.0654	0.2506
C(6)	0.8097	0.2490	0.2519
H(4)	0.560	0.0	0.25
H(2)	0.940	0.115	0.252
H(6a)	0.900	0.302	0.253
H(6b)	0.773	0.268	0.215
H(6c)	0.771	0.266	0.289

[a] The averaged estimated standard deviations are as follows: $\sigma(x) = \sigma(y) = 0.0008$, i.e., 0.008 Å, $\sigma(x) = 0.0004$, i.e., 0.004 Å for the nonhydrogen and hydrogen atoms, respectively, except for those which are fixed.

From the line position in the fast-exchange limit, the equilibrium constant K_{12} can be obtained if the ν_{Si} are known from the slow-exchange regime. A knowledge of both quantities is necessary in order to obtain rate constants in the intermediate exchange regime from the exchange-broadened spectra.

We consider now the case of molecules which form degenerate isomers in the absence of intermolecular interactions. As a consequence, the nuclei A_1 and X_2 will be equivalent as well as the nuclei A_2 and X_1. This situation is, for example, realized in I, where A and X correspond to the pair of nitrogen atoms, to the C(3)/C(5) carbons, or to the methyl carbons. In the solid state the degeneracy of the two isomers will be lifted. Nevertheless, in good approximation the following relation for the chemical shifts will hold:[27]

$$\nu_{A1} = \nu_{X2} \text{ and } \nu_{A2} = \nu_{X1} \quad (3)$$

In the slow-exchange regime the spectra contain then only two lines A_1, X_2 and X_1, A_2 of equal intensity which broaden and sharpen again as k_{12} is increased. In this fast-exchange regime the splitting $\delta\nu = \nu_A - \nu_X$ between the two averaged lines A and X is reduced and given by[23,25]

$$\delta\nu = \Delta\nu(1 - K_{12})/(1 + K_{12}) \quad (4)$$

where $\Delta\nu = \nu_{A1} - \nu_{A2} = \nu_{X2} - \nu_{X1}$ is the splitting on the slow-exchange regime. For the symmetrical case where $K_{12} = 1$ it follows that $\delta\nu = 0$, i.e., lines A and X coincide.

A computer program handling all types of NMR exchange problems has been written to calculate the spectra.[27,28] Note that the line shape theory used here is only valid if rotational sidebands can be neglected. In the presence of the latter more sophisticated techniques have to be used in order to analyze the spectra.[37]

Nuclear quadrupole resonance line shapes were simulated from published solutions[38] of the stochastic Liouville equation for two-site flips of spin-1 nuclei in zero magnetic field. It was assumed that the orientations of the $^{14}N(1)$ and the $^{14}N(2)$ electric field gradient tensors were the same as have been inferred in solid pyrazole,[17] so the flip of a proton from N(1) in one molecule to N(2) in another involves the interchange of the x and the z axes and a change in the quadrupole interaction.

X-ray Crystallography. Compound I crystallizes in the $R\bar{3}c$ space group with cell constants of $a = b = 11.775$ (2) and $c = 20.991$ (4) Å. The crystal structure was determined at room temperature on a CAD4 Enraf-Nonius diffractometer and refined until a final $R = 0.079$.[20] Table I shows the final atomic coordinates for the asymmetric unit.

Results

X-ray Crystallography. The crystal structure can be seen in Figure 2a,b, the first one with the trimeric association around the 3-fold axis and the second one showing the stacking that packs the trimers perpendicular to the c axis.

The crystallographic symmetry imposes a 2-fold axis through the molecules, giving rise to disorder in the N–H proton sites. The trimers are held together by three symmetry related hydrogen bonds (see Table II).

^{14}N Quadrupole Double Resonance Spectra. 3,5-Dimethylpyrazole (I) gave good ^{14}N spectra in cross-relaxation but poor in level crossing, indicating a short T_1 for both nitrogen nuclei; all six lines from two inequivalent ^{14}N nuclei were resolved, enabling reliable assignments to be made. The quadrupole coupling constants e^2qQ/h and asymmetry parameters η derived from these frequencies at room temperature (291 K) are given in Table III and compared with similar values observed in pyrazole (II) at the same temperature.[17] Within the rather poor resolution of cross-relaxation techniques (due to the finite magnetic field in which the spectra are recorded), the number of sets of ^{14}N frequencies given in Table III is consistent with the presence of just one molecule in the crystallographic asymmetric unit.

At first sight, this is not in agreement with the X-ray crystal structure analysis of I which predicts a disordered structure, as noted above. The disagreement would be explained if the three hydrogen atoms in the ring NH···N bonds were undergoing

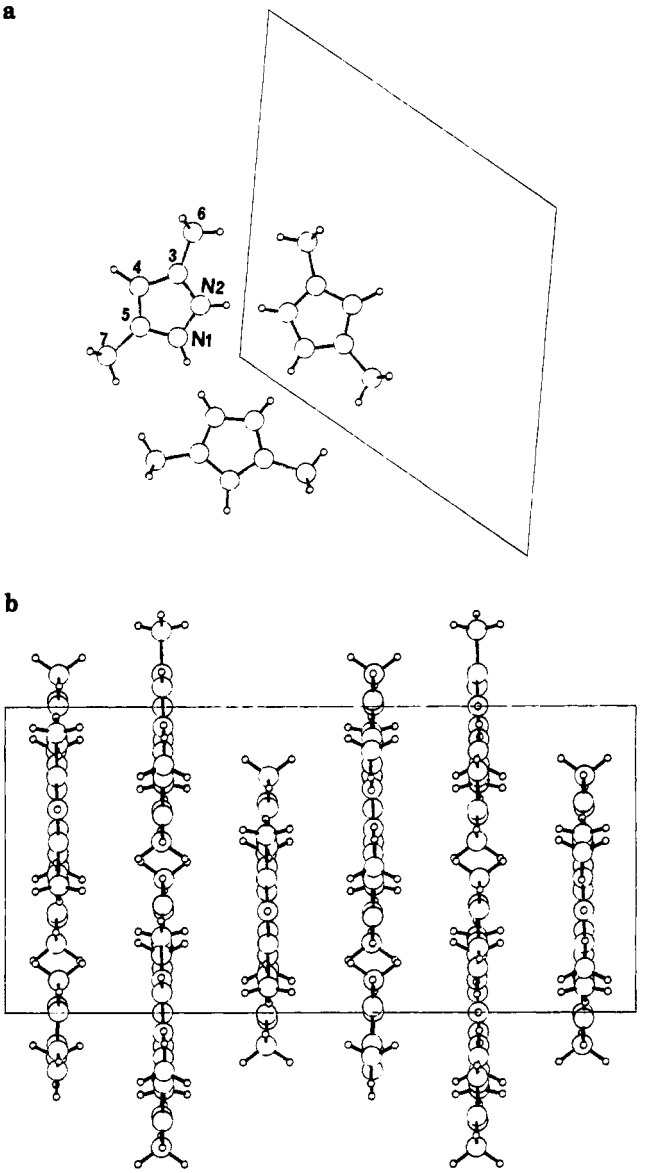

Figure 2. X-ray structure of 3,5-dimethylpyrazole (I): (a) a view of the cyclic trimer projected along the c axis and (b) a molecular packing view projected along the b axis[57] showing the planarity of the trimer.

Table II. Selected Geometrical Parameters (Å, deg) in the Independent Moiety[a]

N(2)–N(1′)	1.334	N(2)–C(3)	1.331
C(3)–C(4)	1.368	C(3)–C(6)	1.491
N(1′)–N(2)–C(3)	109.0	N(2)–C(3)–C(4)	106.2
N(2)···N(1″)	2.977	H(2)···N(1″)	2.10
N(2)–H(2)	0.88	N(2)–H(2)···N(1″)	172

[a] Dashed atoms lie in the symmetry related molecule at $x - y, -y, {}^1/_2 - z$ and double dashed ones at $2 - x, 1 + y - x, {}^1/_2 - z$.

(37) Schmidt, A.; Vega, S. *J. Chem. Phys.* **1987**, *87*, 6895–6907.
(38) (a) Jonsen, P.; Luzar, M.; Pines, A.; Mehring, M. *J. Chem. Phys.* **1986**, *85*, 4873–4880. (b) Meier, P.; Kothe, G.; Jonsen, P.; Trekoske, M.; Pines, A. *J. Chem. Phys.* **1987**, *87*, 6867–6876.

Table III. ^{14}N Quadrupole Resonance Frequencies, Coupling Constants (e^2qQ/h), and Asymmetry Parameters (η) in Pyrazoles at 291 K

compound	atom	obsd[a] ν_z, ν_y, ν_x (kHz)	Zeeman-corrected[31] ν_z, ν_y, ν_x (kHz)	e^2qQ/h (kHz)	η
3,5-dimethylpyrazole[b] (I)	N(1)	1270	1258	2670	0.942
		1387	1374		
		2657	2631		
	N(2)	1790	1773	3705	0.972
		1897	1879		
		3715	3675		
pyrazole (II)	N(1)		1003, 919	2425	0.818
			1323, 1370	2436	0.750
			2315, 2284		
	N(2)		1506, 1500	3756	0.802
			2064, 2087	3783	0.793
			3570, 3587		

[a] By cross relaxation techniques. [b] Level-crossing signals seen at 1245, 1360 (weak), 2582 kHz (N(1)), and 1855, 3592 kHz (N(2)).

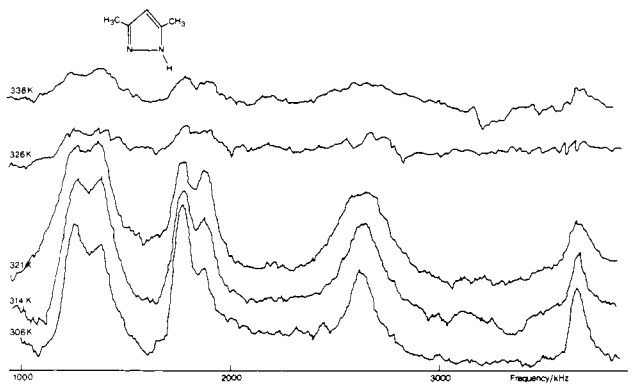

Figure 3. ^{14}N cross-relaxation spectra of 3,5-dimethylpyrazole (I) taken at various temperatures: τ_P = 10 s, τ_{CR} = 1 s.

concerted jumps between the two equivalent positions allowed to them within the hydrogen bond which are too slow at room temperature to affect the ^{14}N quadrupole resonance frequencies. This mechanism is better established by the ^{13}C and ^{15}N magnetic resonance studies, but there is some evidence for its existence in the results of the ^{14}N quadrupole resonance experiments. A series of cross-relaxation spectra taken between 306 and 338 K is shown in Figure 3; at 306 K, all six ^{14}N lines are resolved, as shown in the figure, with a width that is expected in this kind of spectroscopy. As the temperature is raised, the lines begin to broaden by 321 K, particularly ν_x for N(1) near 2630 kHz, as expected for two-site exchange processes (see Experimental Section). Unfortunately, the increasing rate of proton jumping has the effect of shortening the proton spin–lattice relaxation time in low field, so much that above 312 K, the rapid loss of ^1H polarization in the low-field part of the cycle means that the ^1H signal observed in high field is weak and is lost altogether above 338 K, although there are clear signs that the line shifts and broadening are following the expected pattern. Simulations of the experimental line shapes reproduced some of the features in Figure 3, such as the broadening of ν_x for N(1)H and the high-frequency displacement of ν_y, ν_z for the same nucleus as the temperature increased. The pattern of six lines observed at room temperature should eventually collapse to just three, predicted to lie close to 253, 2216, and 2469 kHz if the $^{14}N(1)H$ and $^{14}N(2)$ tensors have the same orientation as has been inferred for solid pyrazole;[17] in agreement with this, the spectrum of I obtained at 338 K shows some evidence for the appearance of a new, weak line near 2200 kHz, but the signal-to-noise ratio is too poor for us to be certain of this finding. In addition, because of the large and variable Zeeman broadening of the cross-relaxation spectra, typically 50–100 kHz for N(1)H signals at 291 K, it has proved difficult to derive reliable values of the exchange rate k_{12} over the narrow range of temperature in which observation was possible. A rough estimate of the corresponding activation energy E_{a12} can be derived by assuming that the additional broadening of the cross-relaxation spectra caused by the proton flips defines a relaxation time T_2^* with an approximately exponential dependence of temperature[39] between 306 and 338 K

$$T_2^* = (T_2^*)_0 \exp(E_{a12}/RT) \quad (5)$$

and a value for E_{a12} of 35 kJ mol^{-1} is thereby deduced, subject unfortunately to an error which is difficult to estimate but could be as large as 15 kJ mol^{-1}. The value for I is not therefore inconsistent with the more reliable figure of 46 kJ mol^{-1} from the ^{15}N studies to be described later.

^{13}C CPMAS NMR Experiments. Since ^{13}C CPMAS NMR experiments do not require isotopically labeled compounds, they have been shown to be useful for a rapid check of whether or not a particular organic compound shows chemical dynamics in the solid state. The latter manifest themselves in the CPMAS NMR spectra of spin 1/2 nuclei by temperature-dependent spectral changes such as line broadening and/or line shifts.[22-28] In favorable cases it is possible to obtain evidence for dynamic processes just by measuring room-temperature ^{13}C CPMAS spectra. Thus, amongst 25 aromatic azoles that are potentially subject to solid-state dynamics[16,19,20,40-42] only one compound, namely, 3,5-dimethylpyrazole (I),[20] showed broad room-temperature ^{13}C CPMAS NMR signals under these conditions. However, this criterion is only qualitative since broadening of ^{13}C CPMAS signals may have different origins, and, generally, experiments at variable temperature are required in order to definitively establish or exclude solid-state dynamics.

Following these lines, low-temperature ^{13}C CPMAS experiments were carried out on I, because of its exceptional behavior.[20] The spectrum obtained at 233 K is shown in Figure 4 (reproduced with permission from ref 20). Five sharp peaks are observed indicating the presence of five inequivalent ^{13}C atoms in I. By contrast, at 303 K only one coalesced methyl peak is observed midway between the low-temperature signals. The two low-field C(3)/C(5) singlets are broadened and nearly coalesced. These spectral changes indicate the presence of a thermally activated process as discussed in Figure 1 which renders the methyl and the C(3)/C(5) carbon atoms chemically equivalent. The rate constant characterizing this process must according to symmetric two-site exchange theory[34] be of the order $k_{12} \simeq \pi\Delta\nu(C(3)/C(5)) \approx 10^3$ s^{-1} at the coalescence point at about 303 K. Since $k_{12} > \pi\Delta\nu(CH_3) \approx 400$ s^{-1}, the coalescence of the two methyl peaks at 303 K is understandable.

In the present study, it is not possible to obtain more reliable rate constants over a wider temperature range. Firstly, $\Delta\nu(CH_3)$ is not much larger than W_0, the line width in the absence of exchange, so a line shape analysis would give accurate kinetic data in a very limited temperature range. The situation for an analysis of the C(3)/C(5) signals in Figure 4 seems better, but unfortu-

(39) Das, T. P.; Hahn, E. L. *Nuclear Quadrupole Resonance Spectroscopy*; Academic Press: New York-London, 1958; p 69.
(40) Faure, R.; Vincent, E. J.; Elguero, J. *Heterocycl.* **1983**, *20*, 1713–1716.
(41) Faure, R.; Vincent, E. J.; Rousseau, A.; Elguero, J. *Heterocycl.* **1987**, *26*, 333–336.
(42) Sanz, J.; Elguero, J., unpublished results.

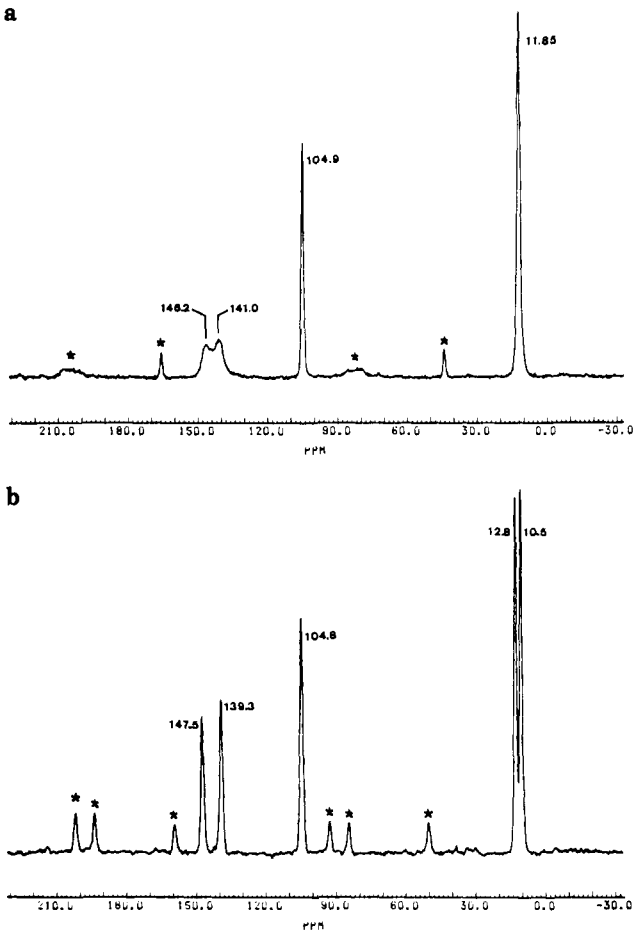

Figure 4. ^{13}C CPMAS NMR spectra of I at 75.5 MHz: (a) at 303 K and (b) at 233 K. Asterisks denote spinning sidebands. Reproduced with permission from ref 20.

nately is complicated by the presence of spinning sidebands, which renders the quantitative analysis of the exchange-broadened line shapes very tedious.[37] Future experiments will use higher spinning speeds. Performing ^{13}C CPMAS spectroscopy in lower magnetic fields may also help, but unfortunately introduces two other problems: the dynamic range is reduced because the value of $\Delta\nu(C(3)/C(5))$ is lower, and the C(3), C(5) line shapes may be significantly affected by residual dipolar interactions with adjacent ^{14}N nuclei.[22]

Variable-Temperature ^{15}N CPMAS NMR Experiments. Since the nitrogen atoms of solid I are directly involved in hydrogen bonding and proton exchange, it is clear that they should be better spin probes for the elucidation of the dynamics in I than the ^{13}C spins. This was one reason for carrying out the above ^{14}N NQR experiments on I. However, high-resolution CPMAS studies cannot be carried out at present on the abundant ^{14}N spins but only on the rare ^{15}N spins which possess spin 1/2. ^{15}N CPMAS NMR experiments have been shown to have a wide dynamic range for studying the kinetics and the thermodynamics of fast proton transfers between nitrogen atoms in solids.[23-28] For sensitivity reasons which are especially severe in the presence of dynamically broadened ^{15}N spectra, the compounds studied have to be enriched with the ^{15}N isotope; for this reason we have, in view of the previous ^{13}C results chosen to synthesize $[^{15}N_2]$3,5-dimethylpyrazole (Ia) and its analogue Ib deuterated on N(1) in order to carry out variable temperature ^{15}N CPMAS NMR experiments. Since the latter were carried out at 2.1 T at spinning frequencies of about 3 kHz, no complications due to spinning sidebands arose.

The experimental and calculated spectra for both compounds are shown in Figure 5, and the kinetic results are assembled in Table IV. At 223 K two sharp lines are observed in the case of Ia (Figure 5a) indicating the presence of two types of nitrogen atom, one protonated (N(1)) and one nonprotonated (N(2)). As

Table IV. Rate Constants k_{12} of the Proton Transfer in Solid $[^{15}N_2]$-3,5-Dimethylpyrazole (Ia) obtained by ^{15}N CPMAS Line Shape Analysis

T/K	k_{12}/s^{-1}	T/K	k_{12}/s^{-1}
263	74	268	130
273	200	275.5	204
286	510	291	679
300	1060	306	1860
346	11000		

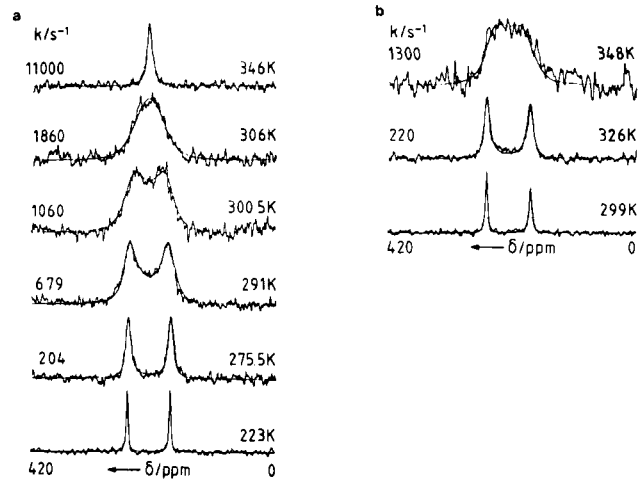

Figure 5. ^{15}N CPMAS NMR spectra of 95% ^{15}N enriched 3,5-dimethylpyrazole (Ia) and of its N(1)-deuterated Ib analogue at 9.12 MHz as a function of temperature: (a) Ia and (b) Ib. The spectra were measured with a Bruker CXP-100 NMR spectrometer equipped with a Doty[33] probe and a home built low-temperature heat exchanger.[23] Experimental conditions: 15 Hz line broadening, 1 K/2 K zero filling, 6–12 ms cross polarization time, 7000 Hz sweep width, 2.3–2.5 s repetition time, 3 μs ^1H-$\pi/2$ pulses, quadrature detection: (a) 236, 15000, 13294, 5406, 3230, and 236 scans from 223 to 349 K and (b) 430, 2874, 2932 scans from 299 to 348 K. Reference: external $^{15}NH_4Cl$. The spectra in Figure 6b were calculated as described in the text. Parameters of the calculation: $\nu_{NH} = \nu_{A2} = \nu_{X1} = 180$ ppm; $\nu_N = \nu_{A1} = \nu_{X2} = 254$ ppm (at 9.12 MHz), i.e., $\Delta\nu = 544$ Hz; (a) $W_0 = 35$ Hz including 15 Hz line broadening; (b) $W_{0_{ND}} = 54$ Hz and $W_{0_N} = 55$ Hz. k is the rate constant. Rotation frequencies were between 2.6 and 3.5 kHz.

the temperature is raised, the two lines broaden and coalesce into one sharp line at 346 K. The position of the coalesced line is described by eq 4. The fact that the line appears in the center of the two low-temperature singlets and does not contain a resolved splitting $\delta\nu$ as defined in eq 4 indicates that all nitrogen atoms have an equal proton density of 0.5, i.e., an equilibrium constant of $K_{12} = 1 \pm 0.07$ for the proton tautomerism. The margin of error of K_{12} is estimated by using eq 4 assuming that a possible splitting $\delta\nu$ less than 20 Hz cannot be resolved. From the low-temperature splitting $\Delta\nu = 544$ Hz we calculate for $\delta\nu = 20$ Hz a value of $K_{12} = 0.93$, which leads to the above maximum error of K_{12} at 346 K. Assuming that the reaction entropy ΔS_{12} of tautomerism is zero it follows from the van't Hoff equation $\ln K_{12} = -\Delta H_{12}/RT + \Delta S_{12}/R$, that $\Delta H_{12} \cong \Delta E_{12} \cong 0 \pm 0.2$ kJ mol^{-1}. ΔH_{12} is the reaction enthalpy and ΔE_{12} the reaction energy of the proton tautomerism. It follows that at 253 K where the lines start to broaden, K_{12} could be of the order of 0.9. Nevertheless, since the margin of error of the rate constants obtained by line shape analysis is anyway of the order of 10%, we have neglected this possible deviation and used a value of $K_{12} = 1$ throughout this study. This assumption is reasonable in view of the satisfactory fit of the experimental to the calculated data as shown in Figure 5. The rate constants obtained can be represented by the Arrhenius equation (Figure 6)

$$k^H_{12} \approx A^H_{12} \exp(-E^H_{a12}/RT), \qquad A^H_{12} \approx 10^{11}, \quad E^H_{a12} \approx 45.7 \text{ kJ mol}^{-1} \quad (6)$$

Because of the relatively small temperature range covered so far

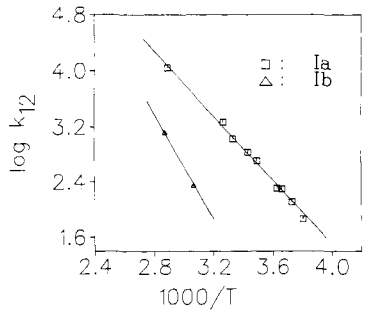

Figure 6. Arrhenius diagram of the triple proton and deuteron transfer in solid 3,5-dimethylpyrazole-$^{15}N_2$ (Ia) and 3,5-dimethylpyrazole-$^{15}N_2$-d_1 (Ib).

the activation parameters in eq 6 might be subject to changes when rate constants can be obtained in the future over a larger temperature range.

In order to know whether or not the tautomerism involves a kinetic hydrogen/deuterium isotope effect we have also performed some preliminary experiments on the deuterated compound Ib as shown in Figure 5. At room temperature the slow-exchange regime is realized. Whereas the width of the low field line is almost as sharp as in the 223 K spectrum of Ia, the high field line is broadened. The broadening allows us to assign this high field line to the N(1) nitrogen. It arises both from a small dipolar coupling with the deuteron which is not completely averaged by MAS[22] because of its quadrupole moment and from a nonresolved scalar ^2H–^{15}N coupling. These effects were taken into account by using a larger value of W_0, the line width in the absence of exchange, for the simulation of this signal. We obtain a kinetic hydrogen/deuterium isotope effect of about 8 at 347 K. At 299 K we estimate from the sharp lines that the rate of deuteron exchange cannot exceed a value of 50 s^{-1}. This leads to a kinetic isotope effect of ≥20 at 27 °C.

Discussion

The results presented in the preceding section show clearly the advantages of combining several different physical techniques to investigate heterocyclic prototropic tautomerism in the solid state.

Firstly the X-ray structure analysis[20] (Figure 2) shows the existence of trimeric units in the solid state with a C_3 symmetry axis, implying hydrogen disorder between equivalent or nearly equivalent configurations but not saying whether the process is static or dynamic. The near or complete equivalence of the disordered structures clearly emerges in the analysis of ^{15}N spectra at elevated temperature, where one collapsed ^{15}N line midway between the two low-temperature ^{15}N lines characteristic for the N(1)H and the N(2) atoms is observed (Figure 5). This signifies an equilibrium constant K_{12} of 1 ± 0.07 so that all nitrogen atoms are attached on average to half a hydrogen atom. Thus, the two potential wells have the same energy within experimental error of the ^{15}N experiments, i.e., the tautomers are degenerate or quasidegenerate. It follows that, in all probability, an isolated 3,5-dimethylpyrazole molecule would be as "asymmetrical" as that of pyrazole;[43] thus, the observed C_{2v} symmetry of a single molecule (∠N1 = ∠N2) is not due to an intrinsic property of the trimer (even if the hydrogen bonds tended to "symmetrize" the geometry) but is a result of disorder due to the superimposition of two equally populated structures.

Secondly, the ^{13}C, ^{15}N magnetic and ^{14}N quadrupole double resonance results for 3,5-dimethylpyrazole (I) show clearly that the disorder is dynamic, in which the protons jump between two potential energy minima with an activation energy of 45 kJ mol^{-1}. The combination of the three magnetic resonance techniques

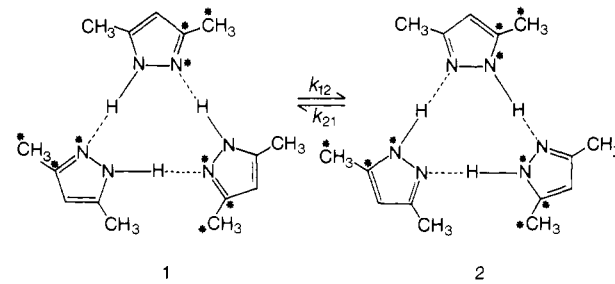

Figure 7. Triple proton transfer in the cyclic trimer of **1** in the crystalline state as established here by a combination of the techniques of NMR, NQR, and X-ray analysis.

enables us to study the dynamics over a temperature range of nearly 100 K from 223 to 338 K and planned measurements of ^{14}N, ^{15}N and ^2H relaxation times at high temperatures as well as polarization transfer experiments at low temperatures will extend the range even further.

Thirdly, the observation of a very large primary hydrogen/deuterium isotope effect for the process leading to the averaged C_{2v} structure for individual 3,5-dimethylpyrazole molecules indicates that this process does not correspond to molecular 180° rotations about an in-plane axis bisecting the N–N bond (process 1 ⇌ 2′ in Figure 1) followed or accompanied by fast proton transfer (process 2′ ⇌ 1′ in Figure 1) but that the latter is the rate-limiting step of the reaction. Thus the simplest explanation of our data is to assume that the rate constants of the processes in Figure 1 are related by $k_{12'} = k_{1'2} = 0$ and $k_{12} = k_{21}$. However, preliminary line shape calculations[28b] based on the more complex exchange model of Figure 1 show that we cannot completely exclude the possibility of slow molecular rotations as in the case of tropolone[21] which could average out small differences between k_{12} and k_{21}. There might also be other molecular motions, such as intermolecular vibrations, librations, or other phonon modes which could assist in rendering the apparent double minimum potential of the proton motion symmetric. However, only the process of proton transfer averages out the chemical shifts between protonated and unprotonated ^{15}N observed in these experiments. Therefore the kinetic isotope effect obtained in this study will always correspond to the proton-transfer step in Figure 1, i.e., to the ratio $k_{12}^{HHH}/k_{12}^{DDD}$.

Thus, by combination of all techniques we can specify the dynamic process in crystalline 3,5-dimethylpyrazole (I) as most likely due to a correlated three-proton jump within the trimer, as shown in Figure 7, characterized by the rate constants $k_{12} = k_{21}$. Although the value of 10^{11} s^{-1} found here for the frequency factor of this process might be subject to changes when kinetic data are obtained over a larger temperature range, one can already say that this value indicates the absence of a large negative activation entropy, in contrast to the value of $\Delta S_{12}^{\ddagger} = -104.6$ J mol^{-1} K^{-1} found for pyrazole exchange in liquid dimethyl sulfoxide solution.[4] Note, however, that in liquid-state studies it is very difficult to define the exchange processes as exactly as in the solid state and to obtain kinetic data which are free from contributions coming from diffusion or preequilibria. Therefore, our data provide the first reliable experimental kinetic data on a known tautomeric process involving a pyrazole derivative. Furthermore, the value of the frequency factor found here is similar to values found recently for intramolecular double proton transfers in solid porphyrins and related compounds,[23-28] where two protons jump along an intramolecular pathway. Thus, the greatest difference between intra- and intermolecular proton-transfer processes seems to be only the fact that the cyclic hydrogen-bonded network in which proton transfers take place is more easily disrupted in the solid state because of the possibility of forming other noncyclic hydrogen-bonded associates. Thus, the finding that the protons in solid I move in a double minimum potential which is symmetric within the margin of error of the ^{13}C and ^{15}N magnetic resonance experiments is a rare finding, especially for intermolecularly exchanging molecules. So far it has been observed in the case of NH···N tautomerism only for porphyrin[26] and *meso*-tetratolyl-

(43) If one compares the intraannular nitrogen angles of pyrazole (II) determined by neutron diffraction (∠N1 = 111.8°, ∠N2 = 104.8°), by microwave spectroscopy (∠N1 = 113.1°, ∠N2 = 104.1°),[44] and theoretically calculated (STO-3G, ∠N1 = 112.5°, ∠N2 = 103.2°)[45] with the calculated values for 3,5-dimethylpyrazole (I) (STO-3G, ∠N1 = 111.5°, ∠N2 = 105.0°)[45] it is safe to assume that the isolated molecules in the gas phase would have quite similar geometries.

porphyrin.[25,28a] In all other porphyrins studied, the double minimum potential was highly asymmetric and strongly dependent on intermolecular interactions, as indeed is also the case for the correlated double proton jumps which occur in many carboxylic acid dimers[46-51] and the $(HCO_3)_2^{2-}$ ion in $KHCO_3$.[31,49,50] In the latter case, there is some evidence that the shape of the potential-energy function changes with temperature, so, for example, the energy difference between the potential energy minima decreases almost to zero as the order parameter decreases.[31] This means that the double minimum potential of a given molecule depends on which well is occupied by the surrounding molecules. By contrast, in I the same activation energy is measured, to within experimental error, over the temperature range from 223 to 338 K, indicating the absence of such interactions in first order.

An interesting feature of the kinetic results is the very large kinetic isotope effect with values of $k_{12}^{HHH}/k_{12}^{DDD}$ of ≥ 20 at 299 K, much larger than those observed for pyrazoles in liquid solution.[3b] This supports the suggestion made above that in the liquid state another process was observed. Unfortunately, it has not yet been possible to establish the rate law of the liquid state tautomerism nor the dependence of rate constants as a function of the deuterium fraction in the mobile NH sites; from such studies further information concerning the liquid-state processes could be obtained.[52-54] Therefore, the kinetic isotope effects established in this study provide the first reliable kinetic isotope effects of the pyrazole tautomerism within an established cyclic hydrogen bonded complex. So far, kinetic isotope effects for a triple proton-transfer reaction have been studied only in the case of the 2:1 proton exchange between acetic acid and methanol in tetrahydrofuran,[52,53] where values of $k_{12}^{HHH}/k_{12}^{DDD} \simeq 10$ were found. These variations are believed to arise from different reaction energy surfaces leading to different proton transfer pathways, different contributions of the heavy-atom motions to the reaction coordinates, and different tunnelling contributions to the reaction rates.[55] Detailed information about the contribution of these various factors could perhaps be obtained by measuring the complete set of multiple kinetic hydrogen/deuterium isotope effects,[52-54] experiments which we intend to perform on solid I by means of a combination of several magnetic resonance techniques. Further structural studies will also be necessary in order to establish the contributions to the kinetic hydrogen/deuterium isotope effects due to changes in the hydrogen-bonded distances upon deuteration, as in the case of disordered O–H···O hydrogen bonds in carboxylic acid dimers.[56]

Moreover, kinetic solid-state measurements enable us to study and analyze the differences in behavior between liquid solution and the disordered and ordered solid state. In the case of pyrazoles, for example, liquid solution studies of annular tautomerism show

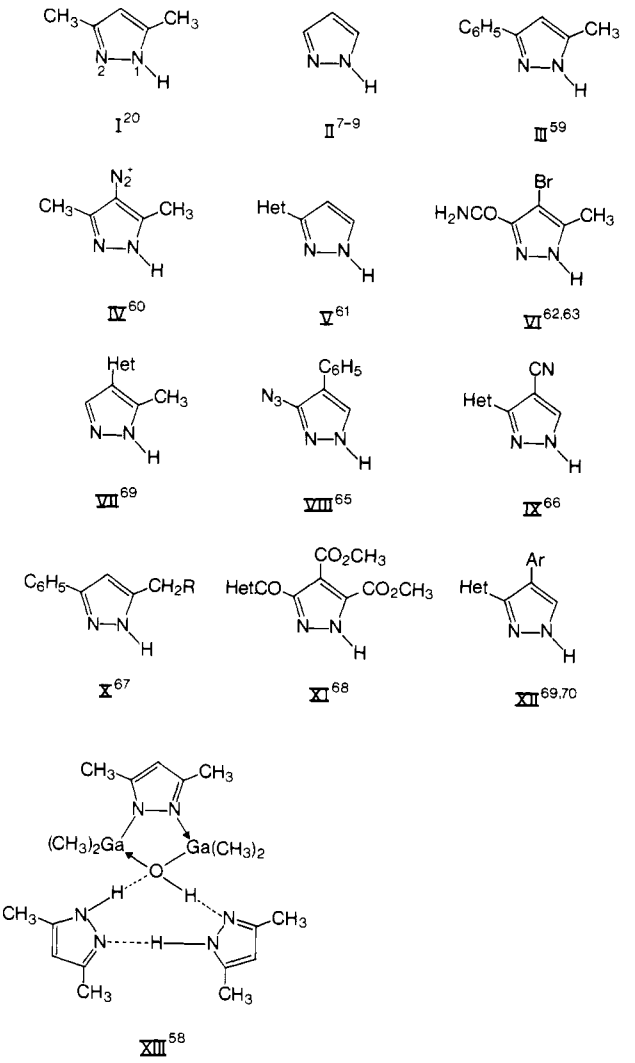

Figure 8. Pyrazoles whose structures have been determined in the solid state (X-ray or neutron diffraction).

Table V.

	$R^3 = R^5$		$R^3 \neq R^5$	
hydrogen atoms ordered	two structures	II, IV	seven structures,	V–XI
hydrogen atoms disordered	two structures	I, XIII	two structures	III, XII

that the activation energy of the process is very sensitive to acid or base catalysis[4,5] but rather insensitive to aliphatic substituents: compare pyrazole II, $\Delta G_{12}^{\ddagger} = \Delta H_{12}^{\ddagger} - T\Delta S_{12}^{\ddagger} \simeq 62$ kJ mol^{-1} (DMSO),[4] $\Delta G_{12}^{\ddagger} \simeq 63$ kJ mol^{-1} (HMPT);[5] 3(5)-methylpyrazole, $\Delta G_{12}^{\ddagger} \simeq 58.5$ kJ mol^{-1} (HMPT);[5] 3,5-dimethylpyrazole (I), $\Delta G_{12}^{\ddagger} \simeq 63$ kJ mol^{-1} (HMPT).[5] In the solid state, in contrast, fast prototropic tautomerism is observed at room temperature in I with $E_{a12} = 46$ kJ mol^{-1} but not in pyrazole II; this is understood if in the latter the tautomeric forms have differing energy, implying that $K_{12} \ll 1$ so that only one form is populated, whereas in the former $K_{12} = 1$ and two forms become equally populated and the protons disordered. To explain such variations, a subtle interplay between inter- and intramolecular interactions must be invoked which leads to different hydrogen bond networks and molecular packings. Information about proton order and disorder in such cases comes from X-ray and neutron crystal structure analysis. A search in the CSD database[57] has yielded 13 different structure

(44) Nygaard, L.; Christen, D.; Nielsen, J. T.; Pedersen, E. J.; Snerling, O.; Vestergaard, E.; Sorensen, G. O. *J. Mol. Struct.* **1974**, *22*, 401–413.
(45) Catalán, J.; de Paz, J. L. G.; Yañez, M.; Mó, O.; Elguero, J., unpublished results.
(46) Graf, F.; Meyer, R.; Ha, T. K.; Ernst, R. R. *J. Chem. Phys.* **1982**, *75*, 2914–2918.
(47) Nagaoka, S.; Terao, T.; Imashiro, F.; Saika, A.; Hirota, N.; Hayashi, S. *Chem. Phys. Lett.* **1981**, *80*, 580–584; *J. Chem. Phys.* **1983**, *79*, 4694–4703.
(48) Schajor, W.; Post, H.; Grosescu, R.; Haeberlen, U. *J. Magn. Reson.* **1983**, *53*, 213–228.
(49) Gough, A.; Haq, M. M. I.; Smith, J. A. S. *Chem. Phys. Lett.* **1985**, *117*, 389–393.
(50) Benz, S.; Haeberlen, U.; Tegenfeldt, J. *J. Magn. Reson.* **1986**, *66*, 125–134.
(51) Jarvie, T. P.; Thayer, A. M.; Millar, J. M.; Pines, A. *J. Phys. Chem.* **1987**, *91*, 2240–2242.
(52) Limbach, H. H.; Hennig, J.; Gerritzen, D.; Rumpel, H. *Far. Discuss. Chem. Soc.* **1982**, *74*, 229–243.
(53) (a) Gerritzen, D.; Limbach, H. H. *J. Am. Chem. Soc.* **1984**, *106*, 869–879. (b) Meschede, L.; Limbach, H. H. *Ber. Bunsenges. Phys. Chem.* **1988**, *92*, 469–485. (c) Limbach, H. H.; Meschede, L.; Scherer, G. *Z. Naturforsch* **1989**, *44a*, 459–472.
(54) Rumpel, H.; Limbach, H. H. *J. Am. Chem. Soc.* **1989**, *111*, 5429–5441.
(55) Bell, R. P. *The Tunnel Effect in Chemistry*; Chapman and Hall: London, 1980.
(56) Agaki, T.; Imashiro, F.; Terao, T.; Hirota, H.; Hayashi, S. *Chem. Phys. Lett.* **1987**, *139*, 331–335.
(57) Allen, F. H.; Bellard, S.; Brice, M. D.; Cartwright, B. A.; Doubleday, A.; Higgs, H.; Hummelink, T.; Hummelink-Peters, B. G.; Kennard, O.; Motherwell, W. D. S.; Rogers, J. R.; Watson, D. G. *Acta Crystallogr.* **1979**, *B35*, 2331–2339.

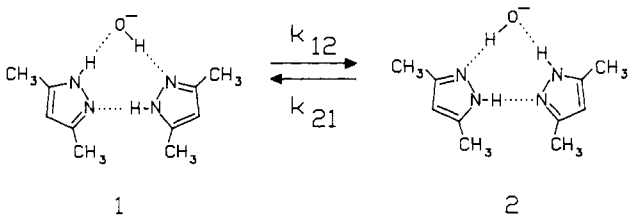

Figure 9. Prototropic processes involved in $Me_2Ga(OH)$–dimepyz–$GaMe_2$·2(XIII).

analyses of 12 pyrazoles, and it is of interest to see how the presence or absence of hydrogen disorder at the temperature of the experiment affects not only the available proton sites but also the averaged structure of the rest of the molecule. It is possible (Table V) to classify the pyrazoles according to the nature of R^3 and R^5 and the location and ordering of the tautomeric proton at the temperature of the structure analysis (see Figure 8 for the formulas and references). In the "ordered" structures (the tautomer represented in Figure 8 being predominant), the mean values for the internal angles corresponding to the nitrogen atoms are ∠N1 = 112.9° and ∠N2 = 104.1° ($\sum\theta$ = 217°, $\Delta\theta$ = 8.8°) independent of whether $R^3 = R^5$ or $R^3 \neq R^5$.

Concerning the three disordered structures whose coordinates are available, I, XIII, and III, different situations are found by X-ray analysis: for compound I, ∠N1 = ∠N2 = 109.0° ($\sum\theta$ = 218°, $\Delta\theta$ = 0°); for compound XIII (two independent 3,5-dimethylpyrazole molecules acting as solvates), ∠N1 = 110.1° and 109.5°, ∠N2 = 107.0° and 107.6° ($\sum\theta$ = 217.1°, $\Delta\theta$ = 2.5°), and, finally, for compound III (two independent molecules), ∠N1 = 109.0° and 109.0°, ∠N2 = 107.4° and 107.8° ($\sum\theta$ = 216.6°, $\Delta\theta$ = 1.4°). It is clear that disorder results in a change in the local molecular point symmetry from C_s to C_{2v} or near C_{2v}. However it is worth comparing the situation found for I and XIII (Figure 9). The refinement of I leads to a "symmetric" solution, ∠N1 = ∠N2, but the refinement of XIII (only the solvation of OH^- by two molecules of I is represented in Figure 9) leads to a 2:1 admixture due to the asymmetry of the OH^- environment, and, as a consequence, $\Delta\theta$ = 2.5°. Work is in progress to confirm the process proposed in Figure 9 by magnetic resonance methods.

Amongst the structures of pyrazoles determined by crystallography, most of them have intermolecular H-bonds, N–H···X, involving substituent heteroatoms. Only four pyrazoles present a network of H-bonds between ring nitrogens (Figure 10).

The case of 3(5)-methyl-5(3)-phenylpyrazole (III) (a tetramer with C_2 symmetry) is of particular interest. One of the major problems in X-ray prototropic studies is the difficulty in locating protons accurately. As X-rays are diffracted by electrons, hydrogen atoms are difficult to locate since they are shifted toward the electron cloud of the non-hydrogen atom to which they are attached. The accuracy of proton location is very dependent on sample, data collection, refinement type, and structure composition. The assignment of peaks in the residual electron density ($\Delta\rho$) as hydrogen atom positions can be tested by careful data selection either at collection time or in the $(\sin\theta/\lambda)$Mx limit used for $\Delta\rho$ calculation and refinement.[71] It is usually assumed that neutron diffraction is superior for proton location.[72] However, in the case of III, both X-ray and neutron diffraction results[59] indicate a "shared" proton situated equidistant from both nitrogen atoms, whereas the ^{13}C CPMAS NMR spectrum corresponds to a unique tautomer.[19] It is not possible to tell in this case, and that of XIII, whether the disordering within the NH···H hydrogen bond is static or dynamic; furthermore, even if an "ordered" configuration is observed at one temperature, this does not exclude the possibility of substantial disordering existing at higher temperatures, when a higher energy configuration becomes appreciably populated (as in the case in some carboxylic acid dimers[46-51]).

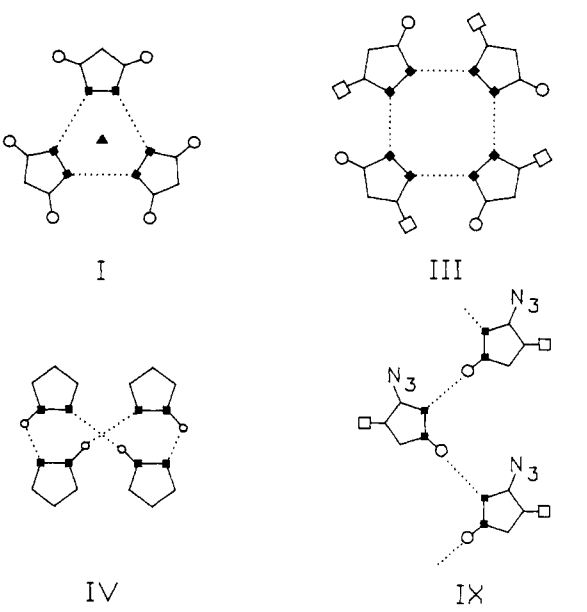

Figure 10. Schematic representation of the H-bond network in some NH···N hydrogen-bonded solid pyrazoles.

As the observed X-ray electron density is an average in time over the experiment and in all unit cells within the sample used, disorder in the proton sites would mean that (i) there are unit cells with molecules which have the proton in one site and there are unit cells with the proton in the other site, supposing it is possible to distinguish both sites, implying that the 2-fold axis is a result of the averaging and that there are "two" types of molecule; or (ii) the actual sample is a twin of just one type of structure, with "one" type of molecule, the twinning generating, when averaged, the 2-fold axis; or (iii) there is just "one" type of molecule, but they exchange a proton many times during the period used for data collection, thereby giving rise to the 2-fold axis; or (iv) the actual situation is a mixture of two or more of the three types of disorder: static, twinned, and dynamic. Distinction amongst these situations is difficult[73] and a combination of X-ray/neutron structure analyses at different temperatures with NMR/NQR techniques is required to resolve the problem.

Conclusions

The combination of ^{13}C, ^{15}N CPMAS magnetic resonance, ^{14}N quadrupole resonance, and X-ray crystallography has enabled us

(58) Rendle, D. F.; Storr, A.; Trotter, J. *Can. J. Chem.* **1975**, *53*, 2944–2954.
(59) (a) Maslen, E. N.; Cannon, J. R.; White, A. H.; Willis, A. C. *J. Chem. Soc., Perkin Trans. 2* **1974**, 1298–1301. (b) Moore, F. H.; White, A. H.; Willis, A. C. *J. Chem. Soc., Perkin Trans. 2* **1975**, 1068–1071.
(60) Brint, R. P.; Coveney, D. J.; Lalor, F. L.; Ferguson, G.; Parvez, M.; Yuen Siew, P. *J. Chem. Soc., Perkin Trans. 2* **1985**, 139–145.
(61) Reimlinger, H.; King, G. S. D.; Peiren, M. A. *Chem. Ber.* **1970**, *103*, 2821–2827.
(62) Foresti, E.; Martelli, G.; Riva di Sanseverino, L. *Atti Accad. Naz. Lincei Rend. Class Sci. Fis. Mat. Nat.* **1970**, *48*, 70–79.
(63) Authors[62] assignment of N(1) and N(2) has been exchanged in order to be consistent with other pyrazoles. The N–H hydrogen atom has not been located.
(64) Fanfani, L.; Nunzi, A.; Zanazzi, P. F.; Zanzari, A. R. *Cryst. Struct. Commun.* **1974**, *3*, 201–204.
(65) Domiano, P.; Musatti, A. *Cryst. Struct. Commun.* **1974**, *3*, 713–715.
(66) Kurihara, T.; Tani, T.; Nasu, K.; Inoue, M.; Ishida, T. *Chem. Pharm. Bull.* **1981**, *29*, 3214–3225.
(67) Kunstmann, R.; Paulus, E. F. *Angew. Chem., Int. Ed. Engl.* **1982**, *21*, 548; *Angew. Chem. Suppl.* **1982**, 1265–1272.
(68) Aliev, Z. G.; Kartsev, V. G.; Atovmyan, L. O.; Voronina, G. N. *Khim. Geterotsikl. Soedin* **1982**, 91–94.
(69) Lang, S. A.; Lovell, F. M.; Cohen, E. *J. Heterocycl. Chem.* **1977**, *14*, 65–69.
(70) Only a figure and a comment about the tautomerizable proton "the proton on the pyrazole ring populates either nitrogen to an indistinguishable extent" are to be found in the publication.[69] The coordinates are not available (Lang, S. A., personal communication).
(71) Huber-Buser, E. *Z. Krist.* **1971**, *133*, 150–164.
(72) Jones, P. E. *Chem. Soc. Rev.* **1984**, *13*, 107–177.
(73) Anson, C. E.; Benfield, R. E.; Bett, A. W.; Johnson, B. F. G.; Braga, D.; Marseglia, E. A. *J. Chem. Soc., Chem. Commun.* **1988**, 889–891.

for the first time to study the dynamics of annular prototropic tautomerism in a substituted pyrazole, namely crystalline 3,5-dimethylpyrazole, in which the most likely mechanism of proton transfer can be established. The compound forms trimers in the solid state held together by NH···N hydrogen bonding, and between 223 and 339 K the evidence is consistent with the tautomerism occurring by correlated triple proton jumps between the two equivalent or nearly equivalent forms of this structure; the rate constant follows the Arrhenius equation with an activation energy of 46 kJ mol^{-1} and a frequency factor of 10^{11} s^{-1}. There is a large kinetic hydrogen/deuterium isotope effect which is temperature dependent, $k_{12}^{HHH}/k_{12}^{DDD}$ being $\geq$20 at 299 K and equal to 8 at 347 K.

Other problems remain, such as the reason for the large isotope effect, and the question of whether or not other mechanisms such as tunneling or molecular librations occur at lower temperatures.[55] It would be important to have more information, both theoretical and experimental, on the shape of the potential energy surface and the effects of deuteration, as we have for the dimer of formic acid.[46] In future work, we hope to study these problems in more detail by means of ^{14}N, ^{15}N and ^{2}H spin-lattice relaxation and line shape measurements and fast field cycling ^{14}N studies at temperatures approaching the melting point.

Acknowledgment. We thank the European Community, the Deutsche Forschungsgemeinschaft, Bonn-Bad Godesberg, the Stiftung Volkswagenwerk, Hannover, and the Fonds der Chemischen Industrie, Frankfurt, the S.E.R.C. (U.K.), and the Pakistan Governments for financial support and research grants. We are also grateful to Dr. Paul Jonsen for a copy of his two-site exchange program, Dr. J. Shaw for performing the calculations, and T. J. Rayner for some of the ^{14}N spectra.

Supramolecular Structure and Microscopic Conformation of Cellulose Esters

Charles M. Buchanan,* John A. Hyatt, and Douglas W. Lowman

Contribution from the Research Laboratories, Eastman Chemicals Division, Eastman Kodak Company, P.O. Box 1972, Kingsport, Tennessee 37662. *Received December 12, 1988*

Abstract: Carbon-13 NMR relaxation studies and two-dimensional nuclear Overhauser exchange spectroscopy (NOESY) have been used to probe the effect of acyl group, temperature, and concentration on supramolecular structure and on the microscopic conformation of cellulose esters. Using these tools we show (i) the basic $^{4}C_{1}$ conformations of the anhydroglucose monomers are not affected by acyl type, temperature, or concentration, (ii) the virtual angle between H1 and H4′ of adjacent anhydroglucose units for cellulose esters is 30–34°, which suggests that these biopolymer derivatives exist as $^{5}/_{4}$ helices, (iii) cellulose triacetate undergoes a unique transition at 53 °C that is likely due to changes in supramolecular structure, and (iv) decreasing concentration induces a complex, interrelated change in both macromolecular order and microscopic conformation.

Cellulose esters have been known since 1869 and have been in commercial production since the first world war. Because of this long history, the art of synthesizing cellulose esters is well established. In contrast, due to the lack of suitable analytical techniques, our understanding of the basic relationships between macroscopic properties and the microstructure of these biopolymer derivatives is not nearly as developed, particularly in relationship to totally synthetic polymers and biopolymers such as proteins and nucleic acids. Application of suitable analytical techniques that would improve our understanding of microstructure of cellulose esters could very well lead to renewed growth in this extremely important class of materials.

Numerous studies have shown nuclear magnetic resonance spectroscopy (NMR) to be an indispensable tool for probing the microscopic behavior of a wide variety of synthetic polymers and biological macromolecules.[1] Recently, we provided NMR spectral assignments for cellulose triacetate (CTA, **1**), cellulose tri-

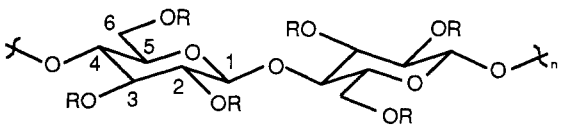

1 R = Ac
2 R = Pr
3 R = Bu

propionate (CTP, **2**), and cellulose tributyrate (CTB, **3**) and described methods by which detailed spectral information about these polymers could be obtained.[2] As a continuation of this work, we have searched for additional NMR techniques by which detailed information about the solution dynamics and conformations of these polymers could be obtained. In this regard, we have found carbon-13 (^{13}C) NMR relaxation time studies to be an excellent tool for probing the molecular dynamics of cellulose esters. In addition, we have coupled two-dimensional (2D) nuclear Overhauser exchange spectroscopy (NOESY) studies with the more established ^{13}C NMR relaxation time technique as a probe of the solution conformations of these macromolecules.

Our strategy in the first part of the work to be presented here was to examine the relaxation time behavior of CTA as a function of solvent, temperature, and concentration. We observed that CTA showed an unusual response to temperature and concentration, prompting comparison of the relaxation time behavior of CTP and CTB as a function of temperature to that of CTA. To determine if the observed changes in relaxation times were due to changes in microscopic conformation (in particular, changes in the virtual angle between adjacent anhydroglucose monomers) or changes in supramolecular structure, we measured the NOESY spectra of CTA, CTP, and CTB. Solution of the peak volume matrices gave the corresponding relaxation matrices at each mixing time for these polymers. The rate constants from these relaxation matrices were then used to calculate interproton distances.

Experimental Section

The preparation of the cellulose triesters and their NMR spectral assignments have been previously reported.[2] The samples were placed in either 5- or 10-mm NMR tubes and degassed by using the freeze-

(1) (a) Bovey, F. A. *High Resolution NMR of Macromolecules*; Academic Press: New York, 1972. (b) Wuthrich, K. *NMR in Biological Research: Peptides and Proteins*; American Elsevier Publishing: New York, 1976.

(2) (a) Buchanan, C. M.; Hyatt, J. A.; Lowman, D. W. *Macromolecules* **1987**, *20*, 2750–2754. (b) Buchanan, C. M.; Hyatt, J. A.; Lowman, D. W. *Carbohydr. Res.* **1988**, *177*, 228–234.

0002-7863/89/1511-7312$01.50/0